Waste Management 53 (2016) 40–54

Contents lists available at ScienceDirect

Waste Management

journal homepage: www.elsevier.com/locate/wasman

Modelling the anaerobic digestion of solid organic waste – Substrate characterisation method for ADM1 using a combined biochemical and kinetic parameter estimation approach

D. Poggio [a], M. Walker [b,*], W. Nimmo [b], L. Ma [b], M. Pourkashanian [b]

[a] Energy Research Institute, School of Chemical and Process Engineering, University of Leeds, LS2 9JT, UK
[b] Energy Engineering Group, Mechanical Engineering, University of Sheffield, S10 2TN, UK

ARTICLE INFO

Article history:
Received 29 February 2016
Revised 21 April 2016
Accepted 22 April 2016
Available online 2 May 2016

Keywords:
Anaerobic digestion
ADM1
Model inputs
Substrate description
Food waste
Green waste

ABSTRACT

This work proposes a novel and rigorous substrate characterisation methodology to be used with ADM1 to simulate the anaerobic digestion of solid organic waste. The proposed method uses data from both direct substrate analysis and the methane production from laboratory scale anaerobic digestion experiments and involves assessment of four substrate fractionation models. The models partition the organic matter into a mixture of particulate and soluble fractions with the decision on the most suitable model being made on quality of fit between experimental and simulated data and the uncertainty of the calibrated parameters. The method was tested using samples of domestic green and food waste and using experimental data from both short batch tests and longer semi-continuous trials. The results showed that in general an increased fractionation model complexity led to better fit but with increased uncertainty. When using batch test data the most suitable model for green waste included one particulate and one soluble fraction, whereas for food waste two particulate fractions were needed. With richer semi-continuous datasets, the parameter estimation resulted in less uncertainty therefore allowing the description of the substrate with a more complex model. The resulting substrate characterisations and fractionation models obtained from batch test data, for both waste samples, were used to validate the method using semi-continuous experimental data and showed good prediction of methane production, biogas composition, total and volatile solids, ammonia and alkalinity.

1. Introduction

The Anaerobic Digestion Model 1 (ADM1) (Batstone et al., 2002) is to date the most comprehensive and widely used model of the anaerobic digestion (AD) process, and describes the main biochemical reactions and physico-chemical processes in anaerobic digestion. Substrate characterisation is ultimately the most influential model input on methane flow prediction (Solon et al., 2015) and a recent review identified that the development of feedstock characterisation methods to provide the required model inputs was still a bottleneck to a broader adoption of ADM1, with more work required in this topic (Batstone et al., 2015).

For each substrate ADM1 requires a physico-chemical characterisation, in terms of its biochemical make-up (carbohydrate, proteins, lipids) and charge bearing compounds (acids, bases, salts). The kinetic characteristics of the substrate (inert content and rapidity of degradation) are also needed as inputs. As well as determining the kinetics of biogas production the substrate characteristics further influence ADM1 predictions in the following ways (Batstone, 2013):

- Gas composition is inherently dependent on the input carbon oxidation state.
- Complex substrates are composed of different fractions which degrade at different rates.
- Buffering compounds (e.g. carbonate and ammonium salts) available in the substrate contribute to the physico-chemical system (e.g. pH) and therefore to many biological inhibition effects.

Two main methods have been implemented for the physico-chemical characterisation: Either from direct analysis of the biochemical fractions (Astals et al., 2013; Koch et al., 2010) or from elemental analysis (Kleerebezem and Van Loosdrecht, 2006; Zaher et al., 2009). However the parameters describing the kinetics of

* Corresponding author.
E-mail address: mark.walker@sheffield.ac.uk (M. Walker).

http://dx.doi.org/10.1016/j.wasman.2016.04.024
0956-053X/

Nomenclature

Where possible we have maintained the nomenclature used in ADM1 in order to facilitate understanding and the reader can refer to both the original ADM1 description (Batstone et al., 2002) for a comprehensive description.

Symbol	Meaning
C_i	carbon content of biochemical fraction (i) in ADM1
f_{ch}	carbohydrate/sugar fraction of substrate
f_d	degradable fraction of substrate
f_{li}	lipid/fatty acid fraction of f_d
f_{pr}	protein/amino acid fraction of f_d
f_s	soluble fraction of f_d
k_{hyd}	hydrolysis constant for particulate fraction
$k_{hyd,r}$	k_{hyd} for rapidly degradable particulate fraction
$k_{hyd,s}$	k_{hyd} for slowly degradable particulate fraction
N_i	nitrogen content of biochemical fraction (i) in ADM1
P_{ka}	acid dissociation constant
P_{kw}	dissociation constant for water
r^2	coefficient of determination
S	soluble substrate concentration
X	particulate substrate concentration
$\overline{y_m}$	average measured methane production
$y_{m,i}$	measured methane production
$y_i(p)$	modelled methane production
α	charge per unit COD for ionic balance
ρ_s	density of substrate
$\sigma_{m,I}$	standard error of measurement

Subscripts

aa	amino acid
ac	acetic acid
an	anion
bu	butyric acid
c	composite organic matter (from biomass decay)
cat	cation
ch	carbohydrate
fa	long chain fatty acids
hyd	hydrolysis
I	inert (non-biodegradable)
IC	inorganic carbon
IN	inorganic nitrogen
li	lipids
pr	protein
pro	propionic acid
s	slowly degradable fraction
su	sugar
r	readily degradable fraction
va	valeric acid

degradation have been usually determined through calibration or parameter estimation (Lübken et al., 2007; Thamsiriroj and Murphy, 2011; Wichern et al., 2009) byt comparing model outputs with experimental data. It has been found, when complex particulate substrates are modelled, that the substrate is best described as composed of several fractions with different degradation rates. In these cases the default formulation of ADM1 needs to be updated to include these new state variables. This has been the approach of some studies (Mottet et al., 2013; Yasui et al., 2008), and in particular the work of Girault et al. (2012) and García-Gen et al. (2015) who developed methods based on batch tests to determine the kinetic fractionation. However both of these methods rely on a visual interpretation of experimental methane production data and therefore introduce some subjectivity to the obtained model parameters.

This paper proposes an improved methodology for substrate characterisation for use with ADM1 involving a combined biochemical and kinetic approach, i.e. based on elemental analysis of the sample and data from bioreactor experiments. Four substrate fractionation models are integrated into ADM1 and evaluated for their ability to describe the anaerobic digestion of source segregated food waste (FW) and green wastes (GW). We aim to remove the subjectivity of existing kinetic fractionation methods by comparing the alternative fraction models using both quality of fit and uncertainty in the calibrated parameters. Furthermore the described methodology, based on data from batch testing, is evaluated and validated using data from semi-continuous the experiments. The proposed methodology is intended to be used to estimate the characteristics of any given substrate to predict the performance of anaerobic processes, including co-digestion.

2. Materials and methods

2.1. Experimental methods

2.1.1. Materials

Household segregated FW and GW were collected at a local recycle centre and stored at 5 °C. Within 24 h, the substrates were examined and large pieces of bone, plastic, metal, wood were removed to avoid damage to the homogenisation equipment and reduce sampling errors during later analysis. The substrates were then homogenised using a mincer to an average particle size of 1 mm, sampled for chemical analysis, and the remaining part was stored at −18 °C and thawed before feeding to the digesters.

2.1.2. Batch tests

Batch tests were carried out in 500 ml laboratory digesters, in triplicate for both substrate and blank (inoculum only), with a working volume of 350 ml. The temperature of the digestion was maintained at 37 °C, to mimic the temperature of a conventional mesophilic AD system, by immersion in a water bath. Agitation was supplied by a vertical stirrer operated at 60 RPM as per the default setting of the equipment manufacturer (Bioprocess Control). The inoculum was obtained from a mesophilic digester treating primary sludge at a wastewater treatment plant. It was screened through a 0.5 mm sieve and then incubated for 4 days in the bottles to allow the degradation of most of the residual easily degradable matter. Before feeding the substrate, the inoculum was sampled for analysis.

The mass of substrate added was calculated on the basis of a defined chemical oxygen demand (COD) based substrate to inoculum ratio (2.5 $gVS_{inoculum}/gCOD_{substrate}$). Thisratio reduces inhibition effects and accumulation of intermediary compounds during substrate degradation (Raposo et al., 2012), therefore allowing hydrolysis rate limiting conditions for methane production from the particulate fractions. After adding the substrate in the digesters, the headspace was purged with pure nitrogen. The produced gas was scrubbed into a 3 M NaOH alkaline solution in order to remove the carbon dioxide and the hydrogen sulphide. The volume of scrubbed gas was then measured through an AMPTSII system (Bioprocess Control), with a resolution of 10 mL. Methane production is reported at STP (0 C and 1 bar) and calculated assuming a scrubber efficiency of 98%, subtracting the concentration of water vapour, and taking into account the overestimation caused from the initial nitrogen content in the headspace, as detailed in

Strömberg et al. (2014). For the latter an approximation of the initial biogas composition is required, and was approximated through the Buswell formula (Rodríguez-Abalde et al., 2013), using the elemental composition of the substrates.

2.1.3. Semi-continuous tests

Semi-continuous tests were carried out in 2400 mL laboratory digesters, in duplicate for each substrate tested. Temperature control, reactor mixing, gas scrubbing and gas volume measurement were performed as in the batch tests. The inoculum was from the same source as for the batch tests. The digesters were manually fed three times a week during the first 80 days, and up to 5 times a week until the end of the experiment, for a total of 45 feeding events during 112 days for GW and 64 feedings during 142 days for FW. Before each addition of substrate, an equal amount of digestate was removed, so to maintain constant the liquid volume inside the digester (2000 mL approximately). Substrates were fed through a hydraulically sealed inlet, therefore minimizing the input of air into the headspace, and without any dilution with water. Organic loads were identical for both substrates, and ranged from approximately 1 to 12 gCOD L^{-1}; the average organic loading rate (OLR) ranged from 0.4 to 7.6 gCOD L^{-1} day. GW experiment was terminated earlier due to repeated foaming events after each feeding which led to blockages in the gas measurement system. Pulsed and irregular feedings of this experimental design allow producing data richer in kinetic information, compared to constant organic loading rate experiments, as it is possible to explore the variation of biogas production with changing concentration of the substrates.

2.1.4. Analytical methods

Substrates, inoculum and effluent from the digesters were analysed for total solids (TS) and volatile solids (VS), volatile fatty acids (VFA), total ammonia nitrogen (TAN), intermediate and partial alkalinity (IA & PA) and pH. Elemental analysis was carried out on substrates and inoculum only. Total solids and volatile solids were measured according to standard methods (APHA, 2005). pH was measured using a pH meter and probe (Hach, CO, USA), and partial and total alkalinity were measured according to Ripley et al. (1986) through titration at pH 5.75 and 4.3 respectively, using an autotitrator (Mettler Toledo).

VFA and TAN were measured on the supernatant obtained through centrifugation of the samples in 2.5 ml vials at 14,000 rpm; in the case of the substrates, a previous dilution with two parts of water was necessary to allow sufficient supernatant to be collected after centrifugation. VFA were determined in a gas chromatography (GC) system (Agilent, CA, USA) equipped with a flame ionization detector (FID) and a DB-FFAP high polarity capillary column (30 m, 0.32 mm ID, 0.5 μm). The in-house method for VFA characterisation was developed as per the manufacturers recommendations; helium was the carrier gas and was adjusted at a flow of 10 mL/min. Each sample was injected automatically with a split ratio of 5:1, and the injection port temperature was 150 °C. The detector temperature was 240 °C, while the oven temperature program was as follows: 60 °C (4 min), ramped at 10 °C min^{-1} to 140 °C, then at 40 °C min^{-1} to 200 °C, remaining at 200 °C for 5 min. Total ammonia nitrogen was measured using a 940 Professional IC Vario ion chromatography (IC) system (Metrohm, Switzerland) as per the manufacturer's instructions.

The Carbon (C), Hydrogen (H), Nitrogen (N) and Sulphur (S) content on TS were determined through ultimate analysis in a Flash EA2000 elemental analyser (CE Instruments, UK) equipped with a Flash EA 1112 flame photometric detector (CE Instruments, UK), according to manufacturer's instructions. The Oxygen content was then calculated by subtracting from TS the sum of C, H, N, S and ash contents, where ash was determined by loss at ignition at 1050 °C.

Methane content was measured with an infrared sensor (Dynament Premier Series sensor), installed in the gas line, with data acquisition performed by an in-house programmed Arduino micro-controller.

2.2. Modelling methods

2.2.1. Modelling of experimental tests

ADM1 was implemented in Aquasim 2.1d (Reichert, 1998) and each experimental test was modelled as a mixed liquid reactor with a gas diffusion link to a mixed gas headspace and a further link to a virtual gasometer (to simulate the accumulated methane volume).

Stoichiometric and kinetic parameters were taken from Rosen and Jeppsson (2006), with the exception of the stoichiometric parameters for proteins which were modified to reflect the protein molecular formula adopted. The disintegration step was only implemented for the biomass decay products, and was omitted in the first substrate degradation step, to avoid an unrealistic two-step solubilisation process as also recently suggested in Batstone et al. (2015).This reduces the correlation between the estimated hydrolysis and disintegration parameters (Rodríguez-Abalde et al., 2013). Therefore the state variable X_c, which is used in the default ADM1 to describe both the substrate and the decayed biomass is maintained only to describe the decayed biomass. As a consequence, the pulse-fed substrate was directly described in terms of its biochemical fractions, and loadings of substrate were implemented in Aquasim as isosceles trapezoidal pulses with a width of 90 s each. Loadings included all COD-fractions and also a further ash fraction (from VS determination) to allow the prediction of inert accumulation in the reactor.

Physico-chemical initial conditions in the reactor were determined from analytical measurements (pH, alkalinity, TAN, VFA, TS, VS, COD_{th}). Initial gas composition in the headspace was assumed to have the same composition of the produced biogas, in congruence with the approach used for calculating the influence of initial nitrogen on methane flow measurements. A description of the method used to estimate the microbial biomass concentrations is given in Appendix A.

2.2.2. Charge balance

Modelling of acid-base reactions requires the solution of a charge balance, which in anaerobic systems assumes the following form:

$$S_{cat} - S_{an} = S_{ac}\alpha_{ac} + S_{pro}\alpha_{pro} + S_{bu}\alpha_{bu} + S_{va}\alpha_{va} + S_{IN}\alpha_{IN} + S_{IC}\alpha_{IC} + OH^- + H^+ \quad (1)$$

where S_{IC} (inorganic carbon fraction, which in solid substrates is almost entirely in the form of hydrogen carbonate) was calculated through PA measurement, with titration to pH 5.75 and then multiplication of the measurement by a 1.25 factor, to take into account that not all hydrogen carbonate is titrated at pH 5.75 (Jenkins et al., 1983); S_{IN} (inorganic nitrogen) in anaerobic systems practically coincides with measured total ammonia nitrogen; concentrations of VFA were directly analytically determined; $H^+ = 10^{-pH}$, $OH^- = 10^{(-pKw+pH)}$ and $pK_w = 14$. The specific charges α_i for each component depend on pH and were calculated as detailed in Nopens et al. (2009). The remaining unknown variables are S_{CAT} and S_{AN} (cations and anions): to remove one degree of freedom, S_{AN} was set to zero when S_{CAT} exceeded S_{AN}, or vice versa. The charge balance is then applied for both the description of the initial conditions and substrate loadings.

2.2.3. Substrate characterisation method

A combined biochemical and kinetic fractionation methodology is used to describe the substrate composition in terms of the various ADM1 state variables (X_{ch}, X_{pr}, X_{fa}, X_l, S_{su}, S_{aa}, S_{fa}, S_{ac}, S_{pr}, S_{bu}, S_{va}, S_l) and their rate of degradation.

2.2.3.1. Theoretical oxygen demand. In ADM1, organic matter transformations are described on a COD basis; therefore, substrate loadings need to be analysed described by their COD content. COD of wastewaters can be determined with high accuracy and with standardized methods; however the application of standard methods to the analysis of solid or semisolid heterogeneous wastes usually produces results with low precision and large confidence intervals, because of non-representative sampling and incomplete COD recovery (Raposo et al., 2008). Optimized methods for the characterisation of solid wastes have been recently proposed, based on "solid dilution" (Noguerol-Arias et al., 2012), but their adoption by the research community has been very limited so far.

In this study an alternative approach was employed and the COD of the substrates was approximated by their COD_{th}, using the measured elemental composition of the substrate. The substrate is considered to be fully oxidised to carbon dioxide and water, with nitrogen reduced to ammonia (as it occurs in anaerobic systems) (Baker et al., 1999):

$$C_nH_aO_bN_c + \left(n + \frac{a}{4} - \frac{b}{2} - \frac{3}{4}c\right)O_2 \rightarrow nCO_2 + \left(\frac{a}{2} - \frac{3}{2}c\right)H_2O + cNH_3 \quad (2)$$

and therefore the specific COD_{th} ($gCOD_{th}/gVS$) is calculated as follows:

$$COD_{th} = 32 \times \left(n + \frac{a}{4} - \frac{b}{2} - \frac{3}{4}c\right) \Big/ molecular\ weight \quad (3)$$

Molecular formulae ($C_nH_aO_bN_c$) of the tested substrates were calculated from the measured elemental composition (Rittmann and McCarty, 2001).

2.2.3.2. Biochemical fractionation. Biochemical fractionation allocates the calculated COD_{th} to the three biochemical compound groups defined in ADM1: carbohydrates/sugars, proteins/amino acids and lipids/fatty acids. It is assumed that different kinetic fractions have the same biochemical fractionation, and therefore only three parameters are defined, namely: f_{ch}, f_{pr}, and f_{li}. These parameters are treated as unknown and calculated through the biochemical fractionation.

The fractionation is based on the following assumptions:

- All VFA is lost during sample preparation (drying) for elemental analysis; therefore all ThOD is allocated to the sum of the particulate and non-volatile soluble fractions (X_{ch}, X_{pr}, X_{li} and S_{su}, S_{aa}, S_{fa}).
- All ammonical nitrogen (S_{IN}) is lost during sample preparation (drying) for elemental analysis, therefore all nitrogen measured in elemental analysis is of organic character and allocated to proteins (X_{pr}) and amino acids (S_{aa}).

The following system of 3 Eqs. (4) and (6) with 3 unknowns (f_{ch}, f_{pr}, f_{li}) allows the calculation of the biochemical fractions, by maintaining a nitrogen, COD and mass balance between the measured substrate and the calculated biochemical fractions:

$$\text{Nitrogen balance}: \quad f_{pr} = \frac{gN_{substrate}}{gCOD_{substrate}} \cdot \frac{gCOD_{pr}}{g_{pr}} \cdot \frac{g_{pr}}{gN_{pr}} \quad (4)$$

$$\text{COD balance}: \quad f_{ch} + f_{pr} + f_{li} = 1 \quad (5)$$

$$\text{Mass balance}: \quad \left(f_{ch}\frac{g_{ch}}{gCOD_{ch}} + f_{pr}\frac{g_{pr}}{gCOD_{pr}} + f_{li}\frac{g_{li}}{gCOD_{li}}\right)\frac{gCOD_{substrate}}{gVS_{substrate}} = 1 \quad (6)$$

The required values for the COD contents ($gCOD\ g^{-1}$ for carbohydrate, protein and lipid) were calculated assigning to each biochemical fraction an ideal molecular formula as shown in Table 1 and calculating its specific COD_{th} (in $gCOD\ g^{-1}$) as in Eq. (3). Carbohydrates were described as polyhexoses with infinite linear chains and lipids as palmitic triglycerides, maintaining the original ADM1 description. In the case of protein, a different molecular formula was used for food waste and green waste, to account for possible differences in COD and nitrogen content; literature data was used to approximate the amino acids content of food waste (Myer et al., 2000) and green waste (Gerloff et al., 1965), allowing the calculation of the respective molecular formulae. Table 1 reports the formula and significant ratios used for the biochemical fractionation. The system of Eqs. (4)–(6) was then solved for f_{ch}, f_{pr}, and f_{li}.

2.2.3.3. Kinetic fractionation. Every substrate was considered as composed of fractions which degrade at different rates. Particulate fractions (X) have by definition hydrolysis as limiting rate and therefore their rate of degradation was described by a first order hydrolysis kinetics (Vavilin et al., 2008). Soluble fractions (S) are directly assimilated by microorganism and therefore their rate of degradation depends on the biomass concentration and their respective uptake rates. In the case of particulate fractions a further distinction was made between readily (X_r) and slowly (X_s) degradable fractions, which can be physically explained by different particle sizes, bioavailability to microorganism colonization, association with recalcitrant polymers (e.g. lignin) or a combination thereof. The hydrolysis rate constants for proteins, carbohydrates and lipids were assumed identical, as the available experimental measurements would not have allowed distinguishing their rate of degradation. The fractionation between soluble, readily and slowly degradable particulate can be modelled by introducing appropriate parameters which map the COD of the substrate onto the respective fractions. The degradable COD is described by a degradable extent parameter f_d which defines the degradable ThOD fraction of the substrate; the non-degradable fraction ($1\text{-}f_d$) is allocated entirely to the inert fraction X_I. The degradable fraction is then considered to be made of a soluble fraction f_s and a particulate fraction ($1\text{-}f_s$). The particulate fraction in turn is allocated into fractions which degrade at different rates, which in the simplest case are two readily and slowly degrading fractions according to another "split" constant (f_{Xr}).

Table 2 shows the four different fractionation models evaluated in this work and the respective parameters which need to be estimated. Table 3 shows the mathematical mappings of the outputs of the biochemical and kinetic fractionation on the ADM1 substrate state variables.

2.3. Model selection and validation

For each substrate, four different fractionation models were tested (Table 2) and the respective quality of fit to the experimental data and uncertainty in parameter estimation evaluated. Mathematical models for biotechnological processes, such as ADM1, include many parameters with uncertain values, and relatively few measured outputs, which in turn makes them hard to calibrate due to structural/practical identifiability issues (Dochain and Vanrolleghem, 2001). Attempts to fit all the parameters simultaneously usually result in very low confidence in the estimated

Table 1
Formulas and significant ratios used for the biochemical fractionation of the substrate.

Biochemical compound	Molecular formula	COD_{th} (gCOD g^{-1} VS)	Nitrogen content (gN g^{-1} VS)	C_i in ADM1 [mol-C g^{-1} COD]	N_i in ADM1 [mol-N g^{-1} COD]
Carbohydrates	$C_6H_{10}O_5$	1.184	0	0.0313	0
Lipids	$C_{51}H_{98}O_6$	2.874	0	0.0220	0
Proteins – GW	$C_{3.95}H_{7.74}NO_{2.06}$	1.285	0.137	0.030	0.0076
Proteins – FW	$C_{3.85}H_{7.64}NO_{2.17}$	1.221	0.136	0.031	0.0079

Table 2
Model descriptions and parameters estimated.

Model nomenclature	Fractionation	Parameters estimated
X	1 particulate (X)	f_d, k_{hyd}
XS	1 particulate (X) and 1 soluble (S)	f_d, f_S, k_{hyd}
XX	2 particulates (X_r and X_s)	f_d, f_{Xr}, $k_{hyd,r}$, $k_{hyd,s}$
XXS	2 particulates (X_r and X_s) and 1 soluble (S)	f_d, f_S, f_{Xr}, $k_{hyd,r}$, $k_{hyd,s}$

Table 3
Mapping of biochemical and kinetic fractionation outputs onto substrate description in ADM1 for XXS model.

Variable	XXS model
S_{su}	$\rho_s COD_{th}\ f_d\ f_{ch}\ f_s$
S_{aa}	$\rho_s COD_{th}\ f_d\ f_{pr}\ f_s$
S_{fa}	$\rho_s COD_{th}\ f_d\ f_{li}\ f_s$
S_{ac}	Measured (GC)
S_{pro}	Measured (GC)
S_{bu}	Measured (GC)
S_{va}	Measured (GC)
S_{h2}	0
S_{ch4}	0
S_{IC}	Measured (titration)
S_{IN}	Measured (IC)
S_I	0
X_c	0
X_{ch}	0
X_{pr}	0
X_{li}	0
$X_{ch,r}$	$\rho_s COD_{th}\ f_d\ f_{ch}\ (1\text{-}f_s) f_{Xr}$
$X_{pr,r}$	$\rho_s COD_{th}\ f_d\ f_{pr}\ (1\text{-}f_s) f_{Xr}$
$X_{li,r}$	$\rho_s COD_{th}\ f_d\ f_{li}\ (1\text{-}f_s) f_{Xr}$
$X_{ch,s}$	$\rho_s COD_{th}\ f_d\ f_{ch}\ (1\text{-}f_s)(1\text{-}f_{Xr})$
$X_{pr,s}$	$\rho_s COD_{th}\ f_d\ f_{pr}\ (1\text{-}f_s)(1\text{-}f_{Xr})$
$X_{li,s}$	$\rho_s COD_{th}\ f_d\ f_{li}\ (1\text{-}f_s)(1\text{-}f_{Xr})$
X_{su}	0
X_{aa}	0
X_{fa}	0
X_{c4}	0
X_{pro}	0
X_{ac}	0
X_{h2}	0
X_I	$\rho_s COD_{th}\ (1\text{-}f_d)$
S_{H+}	Measured (pH)
S_{OH-}	Measured (pH)
S_{cat}	Charge balance
S_{an}	Charge balance
X model: $f_s = 0$, $f_{Xr} = 0$ XS model: $f_{Xr} = 0$ XX model: $f_s = 0$	

parameters. Therefore, only the parameters describing the hydrolysis rate and the substrate kinetic fractionation were selected for calibration, as they are the most sensitive when hydrolysis rate limiting conditions occur. In fact, default microbial uptake kinetic parameters have been satisfactorily used to simulate non inhibiting conditions which happen in batch tests (García-Gen et al., 2015; Souza et al., 2013): in this study, default parameters listed in Rosen and Jeppsson (2006) were used.

Parameters were estimated by a weighted least square method, minimizing the following function (Gujer, 2008):

$$\chi^2 = \sum_{i=1}^{n} \left(\frac{y_{m,i} - y_i(p)}{\sigma_{m,i}} \right)^2 \quad (7)$$

where $y_{m,i}$ is the ith measured value of the target measurement, assumed to be a normally distributed random variable; $y_i(p)$ is the model prediction at the time corresponding to data point I, which could be considered a function of the set of parameters p to be estimated; $\sigma_{m,i}$ is the standard error of the measurement $y_{m,i}$ and weights each term of the sum. The same cost function is implemented in Aquasim in the parameter estimation routine.

In the case of batch tests, the target measurement is the accumulated volume (calculated as the sum of consecutive volume measurements). The standard error of each measurement was calculated by uncertainty propagation as the quadratic sum of all previous errors (Taylor, 1996). Using data from the equipment manufacturer and a conservative approach, each measurement was characterised by a standard error of 0.5 mL. As a consequence, initial volume measurements in batch tests are considered more accurate and have more weight than latter measurements.

In the case of semi-continuous tests, the target measurement is the methane flow rate. Flow rates were calculated from measured volume data points using a backwards difference equation. The standard error of each measurement was calculated by uncertainty propagation for the case of quotients (flow rate as quotient of volume and time interval), which results in the weights in Eq. (7) being proportional to the experimental flow. As a consequence, the cost function will assign similar importance to experimental periods with low flow rate and high flow rate.

The Secant Algorithm (Ralston and Jennrich, 1978) implemented in Aquasim was used as the minimization technique, with a tolerance for convergence of 4E-3 in the objective function. Different initial guesses of target parameters were used in the estimation process to check the convergence of the algorithm towards the same optimum parameters values. Every experimental replicate was treated as a separate data point set for the estimation algorithm, rather than fitting the average of the data points.

The different fractionation models were compared on the basis of their coefficient of determination (R^2), the relative absolute error (rAE), and the standard errors of the estimated parameters. R^2 was calculated as per Eq. (8), where $\overline{y_m}$ is the average of experimental data points, and the rAE was calculated as per Eq. (9). The standard error is calculated by Aquasim as an output of the Secant Algorithm.

$$R^2 = 1 - \frac{\sum_{i=1}^{n} \left(y_{m,i} - y_i(p) \right)^2}{\sum_{i=1}^{n} \left(y_{m,i} - \overline{y_m} \right)^2} \quad (8)$$

$$rAE = \frac{\sum_{i=1}^{n} \left(\frac{|y_{m,i} - y_i(p)|}{y_{m,i}} \right)}{n} \quad (9)$$

The models investigated in this work contain a different number of calibrated parameters and therefore a procedure to compare and select an appropriate one is needed. Two conflicting objectives arise: the goodness of fit and the estimated parameter confidence.

Increasing the number of parameters leads to a closer fit between model predictions and experimental data; at the same time, additional parameters will lead to increased uncertainty, because of correlation between parameters and experimental data being not informative enough (both low quality and quantity of data). In this research for the systematic comparison of different model structures was based on two criteria: (i) Is the maximum relative standard error of the estimated parameters above a certain user-specified threshold (e.g. 10%)? (ii) How good is the fit? The former is used to detect and eliminate those parameter combinations which yield low confidence estimates and the latter is used to rank the parameter combination tested.

3. Results and discussion

3.1. Substrate characterisation and biochemical fractionation

The results of the substrate characterisation for FW and GW samples are shown in Table 4. Both substrates are characterised by a low pH and considerable VFA content, which reflects the partial fermentation process occurred while being stored at the recycling centre. As a consequence, both substrates do not contain any carbonate buffer (partial alkalinity).

Elemental analysis of the samples resulted in the following molecular formulas: $C_{17.0}H_{30.1}N_1O_{8.7}$ for FW and $C_{20.4}H_{31.6}N_1O_{12.1}$ for GW. COD_{th} was then calculated for each substrate and used, along with the formulas and ratios shown in Table 1, to solve Eqs. (4)–(6), yielding the biochemical fractionation results shown in Table 5; fractions are reported both on a COD and VS basis. Table 6 reports the remaining ADM1 state variables used to describe the substrates, including the results from the charge balance equation (anion and cation concentrations).

It is difficult to compare the substrate composition results with other studies, given the geographical and temporal variations of these kinds of waste. However, an important observation about the calculated lipid content needs to be made. In fact, in the case of GW lipid content (12.8% on a VS basis) is higher than the reported amounts from other databases or publications; e.g. from consulted entries in a comprehensive biomass database (ECN/Phyllis), averages values around 5% are found. Two reasons can explain the difference:

Table 4
Characterisation of source segregated food and green wastes.

Analysis	Units	FW	GW
TS	g kg^{-1}	296.5	401.7
VS	g kg^{-1}	274.4	274.6
Ash (at 1050 C)	% TS	7.5	31.6
C	% TS	48.8	34.7
H	% TS	7.2	4.5
N	% TS	3.3	2.0
S	% TS	0.10	0.03
O	% TS	33.1	27.2
COD_{th} of VS	gCOD g^{-1} VS	1.61	1.42
COD_{th} of substrate	gCOD g^{-1} substrate	0.44	0.39
pH	n/a	4.74	5.02
Partial Alkalinity	mg $CaCO_3$ kg^{-1}	0	0
Intermediate Alkalinity	mg $CaCO_3$ kg^{-1}	3443	3181
Total Ammonia Nitrogen	mg N-NH_4 kg^{-1}	528	630
VFA			
Acetic	mg kg^{-1}	3029	4173
Propanoic	mg kg^{-1}	27	223
i-butyric	mg kg^{-1}	19	12
n-butyric	mg kg^{-1}	53	136
i-valeric	mg kg^{-1}	0	25
n-valeric	mg kg^{-1}	2	8

Table 5
Fractionation of substrate into biochemical compounds.

	Units	FW	GW
COD_{th} from elemental analysis	gCOD g^{-1} substrate	0.440	0.391
COD_{th} from VFA and alcohols	gCOD g^{-1} substrate	0.013	0.006
Total COD_{th}	gCOD g^{-1} substrate	0.453	0.397
Fractionation of COD_{th} from elemental analysis			
Carbohydrates (f_{ch})	% COD_{th}	36.3%	54.7%
Proteins (f_{pr})	% COD_{th}	20.2%	19.1%
Lipids (f_{li})	% COD_{th}	43.5%	26.2%
Fractionation of total VS			
Carbohydrates	% VS	47.8%	64.6%
Proteins	% VS	25.7%	20.7%
Lipids	% VS	23.6%	12.8%
VFA and alcohols	% VS	2.9%	1.9%

Table 6
Substrate description based on charge balance.

ADM1 state variable	Units	FW	GW
S_{ac}	gCOD L^{-1}	3.241	4.465
S_{pro}	gCOD L^{-1}	0.040	0.251
S_{bu}	gCOD L^{-1}	0.132	0.147
S_{va}	gCOD L^{-1}	0.004	0.032
S_{in}	M	0.030	0.036
S_{ic}	M	0	0
OH^-	M	4.42E-10	8.42E-10
H^+	M	1.82E-05	9.55E-06
S_{cat}	M	0	0
S_{an}	M	0.012	0.004

- Potential contamination with cooking oil (household collections make part of the green waste).
- Influence of lignin content, which has COD:mass ratio of 1.56; considering a ratio of 1.18 for carbohydrates and 2.87 for lipids, it is evident how the presence of lignin would shift the biochemical fractionation towards a higher content of lipid (while proteins are directly determined by the N content).

Notwithstanding the possible influence of contamination, the aforementioned influence of lignin is theoretically valid and shows a limit of the proposed method: in the case of substrates which have a relatively high content of lignin, the results will have an artificially higher content of lipids. While the COD balance and C:N ratio are still correctly maintained, an artificially higher concentration of lipids will affect some metabolic interactions in ADM1, such as: higher content of slowly consumed fatty acids, amount of hydrogen produced from fatty acid oxidation, biased parameter values when fatty acid inhibition is implemented and calibrated. An alternative is to directly measure the lignin content and allocate it fully to the inert fraction, as done by Koch et al. (2010). However the procedure would become more time-consuming.

3.2. Kinetic fractionation using batch data

Results of the estimation of initial conditions are included in the Appendix A. The parameters estimated for the kinetic fractionation of both substrates are shown in Table 7. The experimental data and simulated curves (using the four fractionation models X, XS, XX, XXS) for the accumulated methane in batch tests are shown in Fig. 1.

In general, an increase in the complexity of the model, related directly to the number of parameters calibrated, corresponded to a better fit to the experimental data. This can be seen visually in Fig. 1 and also quantitatively by a higher R^2 and lower rAE. This is to be expected in the case of nested models, where the model with more parameters can better adapt to the experimental data.

Table 7
Results of model parameter estimation using batch test data, including parameter values, standard errors and quality of fit.

Feed	Model	Parameter values					Standard errors (%)					rAE	R^2
		f_d	f_S	f_{Xr}	k_{hyd_r}	k_{hyd_s}	f_d	f_S	f_{Xr}	k_{hyd_r}	k_{hyd_s}	(%)	(%)
GW	X	0.300				0.682	1.5				4.7	7.4	98
	XS	0.327	0.255			0.296	0.9	3.3			4.3	4.3	99.1
	XX	0.326		0.451	1.57	0.192	2.2		8.1	13.4	14.3	4.3	99.1
	XXS	0.344	0.212	0.44	0.68	0.136	1.8	5.3	26.4	25.9	25.9	3.9	99.2
FW	X	0.747				1.09	0.8				3.1	7.2	96.9
	XS	0.811	0.332			0.37	0.8	3.2			4.5	5.5	98.1
	XX	0.897		0.541	2.54	0.13	1.7		2.4	6.4	9.0	3.4	99.5
	XXS	0.905	0.156	0.499	1.48	0.12	1.6	7.6	3.3	8.5	11.8	3.0	99.4

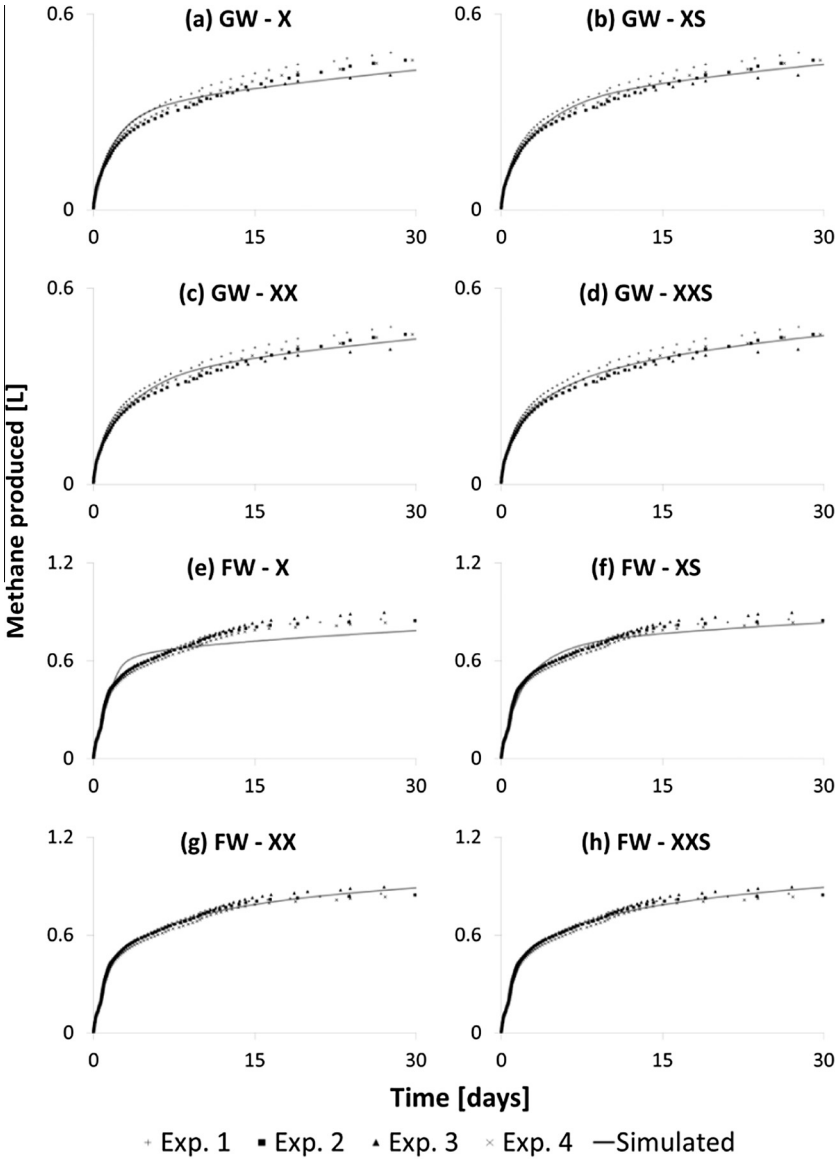

Fig. 1. Batch test data for GW and FW with best fitting model output for X, XS, XX and XXS models.

However, the increase in complexity also corresponded to an increase in the uncertainty of the estimation of the parameters, as given by their calculated standard errors.

In the case of green waste, the X model was able to achieve a good fit to the experimental data using a single particulate fraction, as indicated by a rAE of 7.4% and R^2 of 98%. The more complex model XS increased the quality of fit (rAE 4.3%), while maintaining comparable standard errors in the estimated parameters (maximum errors: 4.7% for model X, and 4.3% for model XS). Increasing the model complexity to XX and XXS resulted in a small increase in fit quality (rAE 3.9%), while the uncertainty in the parameters increased to a maximum of 14.3% and 26.4% respectively. High values of standard errors are related to the experimental data not being sufficiently rich and also indicate low sensitivity cost

function to the optimal parameters. Therefore, in the case of GW, the XS model would be the recommended fractionation model, as it allows good quality of fit with acceptable parameter uncertainty.

For food waste, it is graphically evident that to achieve a good fit with the experimental data at least two particulate fractions are needed. The model fit for the X and XS models, as shown in Fig. 2e and f, displays the inadequacy of the single particulate fraction with first order kinetics in replicating the more complex kinetics of food waste degradation; goodness of fit rAE is at 7.2% and 5.5% for X and XS models respectively. Where two particulate fractions are assumed, a readily and slowly degradable fraction, the characteristic shape of the methane production can be replicated, and the rAE accordingly decreases to 3.4% and 3.0% for XX and XXS model, respectively. The XX model would be the recommended fractionation model, as it gives similar good quality of fit compared with XXS but with lower parameter uncertainty.

In both substrates, there is an increase in the value of f_d with model complexity. In fact, with more complex models the calibration is able to take into account also the less precise volumes measurements towards the end of the experimental period, while with simpler models the calibrated parameters is mainly determined by the more precise initial data.

3.3. Semi-continuous experiments

The laboratory digesters were fed the equivalent OLR, on a COD_{th} basis, as presented in Section 3.1, of GW and FW, respectively. Despite the equivalent loadings the methane production kinetic and volume were different due to the different compositions and degradability of the organic wastes. FW had higher methane production than GW, mainly due to higher degradability and rate of degradation. For the GW and FW fed systems respectively, the average methane volumetric productivity over the course of the experiment was 0.17 and 0.60 L $L^{-1}_{digester}$ day^{-1} and the specific (methane) yield was 0.123 and 0.280 L g^{-1} COD_{added} (0.175 and 0.449 L g^{-1} VS_{added}).

The methane production rate and the organic loading pulses for the GW and FW digesters are shown in Fig. 2. While GW experiment was terminated earlier due to repeated foaming events, at OLR between 3 and 4 gCOD L^{-1} day^{-1}, no excessive production of foam was observed in the FW system, despite the higher OLR over later parts of the experiment; instead the digester showed the initial signs of organic stress with an increase in the VFA concentration to around 4 gCOD L^{-1}, at an average OLR of 9.5 gCOD L^{-1} day^{-1}. Higher TS content in the GW reactor could have led to higher viscosity and therefore a higher tendency to foam.

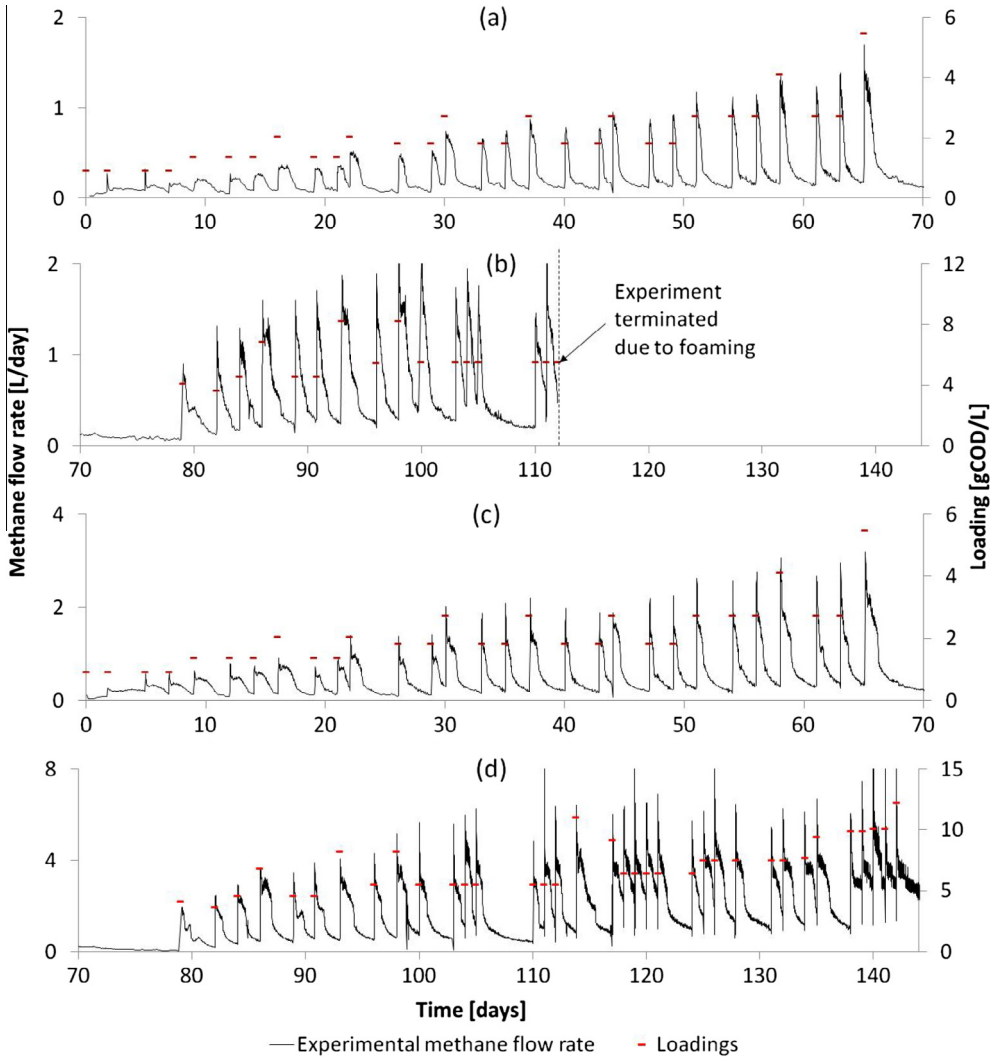

Fig. 2. Overview of the experimental methane production from the semi-continuous 2-l laboratory digester fed with GW (a) and (b), and FW (c) and (d).

3.4. Kinetic fractionation using semi-continuous data

The methane production data collected in the semi-continuous testing was used to estimate the kinetic and fractionation parameters and identify the most appropriate fractionation model (X, XS, XX, and XXS) for both FW and GW. Calibrated kinetic parameters are shown in Table 8, together with standard errors and goodness of fit indicators and these values can be compared with the equivalent results from the batch testing shown in Table 7. Similarly to batch tests, more complex models resulted in better fit. In GW fractionation, the coefficient of determination R^2, increased from 79.8% for model X, to 93.3 % for model XXS; in FW fractionation R^2 increased from 74.0% for model X to 90.0% for model XXS. The parameter uncertainty remained low in all cases indicating that the dataset was sufficiently rich to allow independent estimation of each parameter. The exception to this was in the application of the XXS model to the GW data which resulted in a maximum error of 9.7%.

Fig. 3 shows an example of a response of the systems to a pulse load of GW and FW, demonstrating the comparative ability of the four fractionation models to describe the methane production kinetics. This figure is indicative of the fit over the whole experimental period except the early stages and final stages during which less good fit was observed (Fig. 4), probably due to the effects of microbial acclimatisation and inhibition respectively, which will be discussed separately.

Fig. 3a allows the following observations with regard to the GW fractionation; The X model tends to underestimate both high flow and low flow data points. The introduction of a further particulate fraction in XX model improves noticeably the fitting. The introduction of the soluble fraction in XS model improves the fitting of the high flow data points, i.e. shortly after a feeding event, compared with the X model, while the fitting at the end of the feeding period remains less accurate. XXS model is practically identical to XX model, as shown in the R^2 and rAE values in Table 8, but with the disadvantage of higher parameter uncertainty. This indicates that GW is better described by two different particulate fractions which degrade at different rates (XX model) and that the soluble (non-VFA) fraction in green waste is not phenomenologically important. This is in contrast to the results of the batch tests, on the basis of which the XS model was recommended. Based on the results of the semi-continuous testing the XX model would be selected considering the quality of fit and parameter uncertainty.

Regarding the FW fractionation models, the results of which are shown in Fig. 3b, the following observations can be made; The X model, similarly to GW, tends to underestimate both high flow and low flow data points. The introduction of a soluble fraction (XS) allows better reproduction of the peak biogas production directly after the feedings, although the fitting in the remainder of the profile is less accurate. In XX model the profile is better simulated, but the high flows after the feedings are underestimated. XXS model is finally able to give the best fit both in the high and low flow sections. It can be concluded that food waste is better described through a fractionation that includes a soluble fraction (15% of the degradable COD) and two particulates having a similar share of degradable COD and different rates of degradation (differing one order of magnitude).

Compared to the middle stages of the experiment, the quality of fit in the early stages is poor for all the fractionation models, as shown in Fig. 4a and b. Large deviations between experimental and modelled data are evident, with experimental flows showing an almost flat profile unresponsive to substrate additions. This can be attributed to the inoculum not being acclimated to the organic makeup of the substrates fed, lacking the adapted hydrolysing enzymes. Acclimatisation of the inoculum and its influence on the calibrated parameter values has been shown also by Girault et al. (2012) while in the method proposed by García-Gen et al. (2015), a series of 6–8 repeated batches is implemented and the methane production of the last batch is used for calibration. Another explanation could be a low initial biomass/substrate ratio during the initial stages of experiment: in fact it has been shown that concentration of biomass influences the hydrolysis rate (Jensen et al., 2009) and first order hydrolysis is an adequate description only when the substrate is fully colonized by the bacteria. Modification to the hydrolysis function in ADM1 (e.g. Contois instead of first-order) could address this issue to improve the model predictions during inoculum adaptation.

In the final stages of the experiments, at higher loading rates, the model quality of fit tends to decrease again, as shown in Fig. 4c and d. Non-monotonic curve is evident in Fig. 4c. This can be attributed to biochemical inhibition phenomena becoming more important, and therefore the methane production was no longer hydrolysis limited. The effect is more pronounced in the FW tests, which showed other indications of organic stress in the form of an increase in VFA concentration. Possible inhibiting effects are due to transient variations of inhibiting compounds, such as VFA and long chain fatty acids (LCFA) which reduce various microbial uptakes reactions. The original ADM1 version (Batstone et al., 2002) implements VFA inhibition implicitly as pH inhibition, while LCFA is not implemented. Therefore the disagreement in model predictions can be attributed to either inhibitions mechanisms not being implemented or inhibition parameters not accurate; both were outside the scope of this work.

3.5. Assessment of batch vs. semi-continuous based kinetic fractionation

Standard errors of calibrated parameters were lower when using semi-continuous rather than batch data meaning that calibrated parameters have a better identifiability: average standard error in of all GW fractionations is approximately 2%, with maximum of 9.7% (compared to an average of 10% and maximum of 26.4% using batch data); in FW fractionation, average is approx.

Table 8
Results of model parameter estimation using semi-continuous experimental data including parameter values, standard errors and quality of fit to semi-continuous test data.

Feed	Model	Parameter values					Standard errors (%)					rAE	R^2
		f_d	f_{Xr}	k_{hyd_r}	k_{hyd_s}	f_S	f_d	f_{Xr}	k_{hyd_r}	k_{hyd_s}	f_S	(%)	(%)
GW	X	0.330			1.42		0.6			1.3		24.5	79.8
	XS	0.350			0.97	0.167	0.6			1.6	3.1	21.8	86.7
	XX	0.380	0.514	4.75	0.19		0.4	0.7	1.6	2.8		13.1	93.1
	XXS	0.383	0.495	5.62	0.19	0.049	0.3	0.8	2.0	2.4	9.7	13.0	93.3
FW	X	0.766			1.16		0.2			0.6		50.8	74.0
	XS	0.783			0.77	0.197	0.2			0.8	1.2	44.7	81.0
	XX	0.846	0.492	5.98	0.24		0.2	0.4	1.0	1.3		35.1	85.0
	XXS	0.848	0.484	3.22	0.21	0.152	0.1	0.6	1.4	1.4	3.5	30.0	90.0

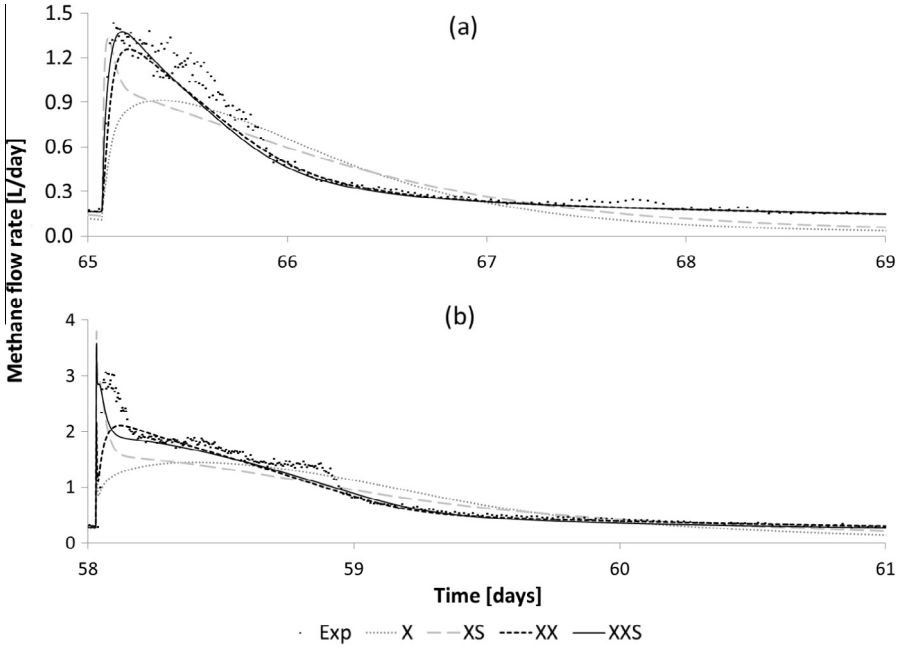

Fig. 3. Comparison of best model outputs (X, XS, XX, XXS) with experimental methane flow from GW digestion for the pulse loading occurring at 65 days for GW (a) and 58 days for FW (b).

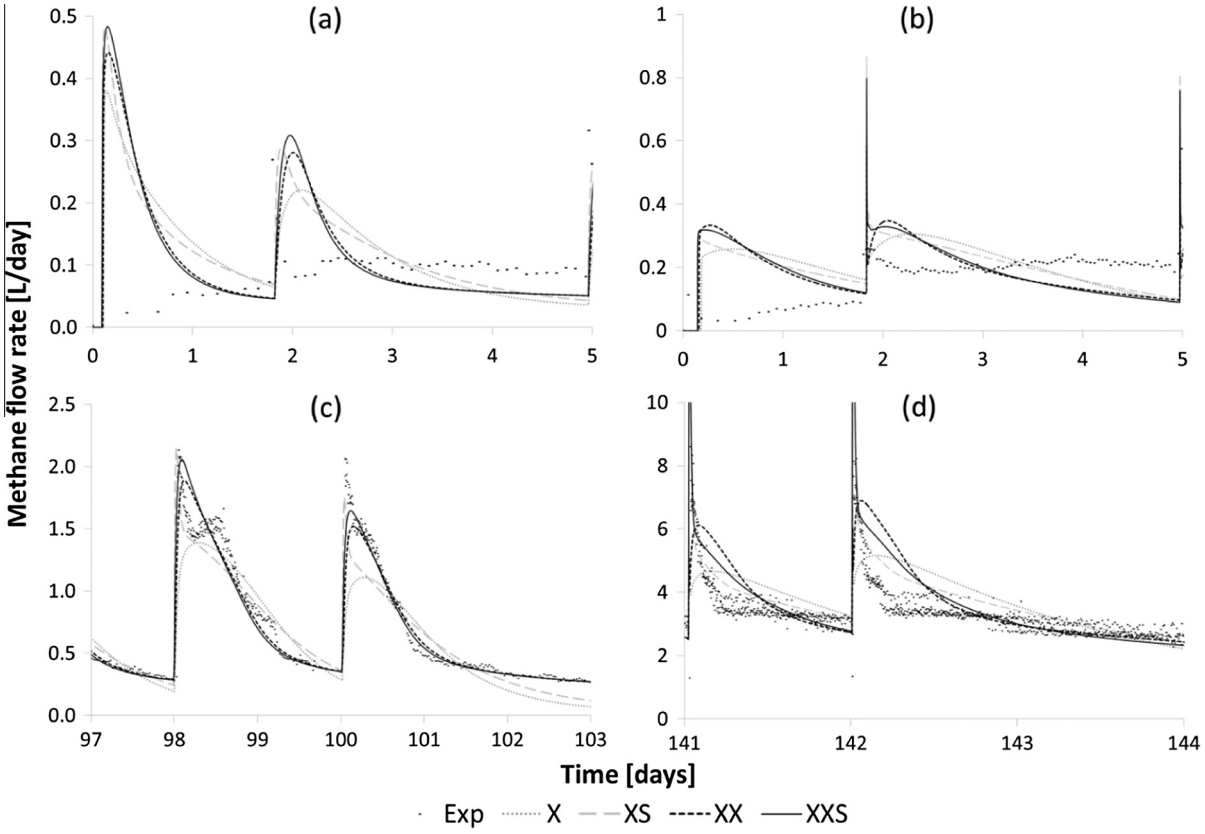

Fig. 4. Comparison of best model outputs (X, XS, XX, XXS) with experimental methane flow for periods 0–5 days for GW (a), and FW (b), 97–103 days for GW (c) and 141–144 days for FW (d).

1%, with maximum of 3.5% (compared to an average of 5% and maximum of 11.8% using batch data). The difference is due to the much higher number of data points and feeding events in semi-continuous experiments, which overall produced a more informative data set. Semi-continuous estimation also increases the differences in goodness of fit between alternative fractionations: in the case of GW, XX fractionation now also appears better suited than XS, while they appeared equivalent from batch estimation.

Regarding the values of the calibrated parameters, different observations can be made: The extent of degradation (f_d) remained similar batch and semi-continuous tests, with a slight increase for the GW semi-continuous test, with an average increase of 11% across the various fractionations. Similarly, the parameter f_{Xr} showed small variations between the tests, and remained within the range 0.44–0.54 for GW, and 0.49–0.54 for FW. The parameter f_S showed bigger variations, especially in the case of GW with higher values obtained in batch tests (ranges 0.21–0.25 in batch and 0.05–0.16 in semi-continuous). Hydrolysis constants displayed noticeable variations: much higher values in semi-continuous tests, with a marked increase in GW (2–5 times higher depending on the fractionation model used, compared with batch tests) and twice as higher in FW (with only X fractionation maintaining similar values). The main reason for this difference appears to reside in the adaptation of the microbial biomass to the substrate. The observations of increased kinetic parameters between batch and continuous operation are in agreement with other similar works (Batstone et al., 2009).

3.6. Validation of batch based substrate fractionation

Validation of the substrate fractionation methodology was performed by comparing the semi-continuous experimental data to the model prediction with parameters calibrated using batch experimental data using the chosen model structures from Section 3.2, i.e. XS for GW and XX for FW and parameter values as per Table 7. This was done using experimental data for the instantaneous methane production, the time-averaged specific methane yield, and from the offline analyses performed.

3.6.1. Methane production

For the instantaneous methane production, in the case of GW the rAE and R^2 values were 30.6% and 81.7% (c.f. 13.1% and 93.1% from Table 8) and for FW were 35.0% and 85.0%, respectively (c.f. 30.0% and 90.0% from Table 8). Specific yields were calculated as the average ratio of the methane produced over the amount of volatile solids fed in six consecutive feedings, while volumetric productivity was calculated as the amount of methane produced per unit of digester volume in the interval of time between two feedings. In the case of specific methane yield the rAE value for GW was 19.9% for batch and 12.1% for semi-continuous. For FW the rAE was 10.9% for batch compared with 11.5% for continuous.

This shows that the batch based fractionation method is suitable when the modelling objective is prediction of time averaged methane production rather than instantaneous. The relatively poorer prediction of instantaneous methane production follows from the large differences in kinetic parameters between batch and semi-continuous calibration as discussed in Section 3.5. Fig. 5 shows the specific methane yield over the experimental period for both GW and FW and in both cases the trend is followed.

3.6.2. Other offline analyses

As well as the methane production rate which formed the basis of the substrate fractionation method several other measurements were taken during the semi-continuous tests and can be compared with the simulated outputs. Figs. 6 and 7 show these comparisons for GW and FW, respectively.

Total and volatile solids are important variables for prediction since they are proxies for unconverted degradable matter still available in the effluent, can influence engineering aspects such as reactor mixing and digestate pumping, downstream equipment (e.g. solid/liquid separation), and influence mass transfer processes in the reactor (Abbassi-Guendouz et al., 2012). In both GW and FW experiments, total and volatile solids increased during the test as shown in Figs. 6a and 7a respectively, caused by the accumulation of inerts and slowly degradable particles. FW simulations achieve significant goodness of fit (rAE 7%) for TS, while VS is underestimated in the first part of the experiment, resulting in a higher error (rAE 18%). In the case of GW is noticeable an increasing error in the prediction of TS, indicated by a relatively high rAE of 19%. Sampling errors and incomplete mixing could contribute significantly to these errors especially in the GW test where the digestate became more heterogeneous as the experiment progressed.

Total ammonia nitrogen has direct influence on the inhibition of many microbial processes, and therefore it is important that the model can reproduce the experimental values. As shown in Figs. 6b and 7b, the experimental trend is again of a constant increase in concentration: from an initial 1.4 g N-NH_4 L^{-1} to final values of 3.5 and 1.7 g N-NH_4 L^{-1} in FW and GW by the end of the tests. The higher increase of TAN in FW is caused by higher nitrogen content and substrate degradability. Goodness of fit was very good for FW (rAE 5%), which validates the value of the calibrated extent of degradation for the protein content in FW. In the case of GW the simulation slightly overestimates the experimental values (rAE 12%) by the end of the experiment.

Bicarbonate alkalinity (BA) is the main buffer in anaerobic systems, reducing changes in pH following VFA production: its measure indicates resistance to organic overload and together with VFA is the main indicator of process stability (Steyer et al., 2006). A BA accurate prediction is therefore important as it is related to the overall prediction accuracy of pH changes and process stability. The model predictions for GW and FW are shown in Figs. 6c and 7d respectively. Experimental values show an initial trend of increasing BA, especially for FW tests. In this case the above-mentioned increase in TAN corresponds to an increase in positive charges (inorganic nitrogen mostly in the form of ion ammonium NH_4^+, with $pK_a = 9.25$) which in turn allows a higher amount of the negatively charged bicarbonate ion HCO_3^- to remain in solution (and not being transformed into gaseous CO_2). In the case of FW test, there is a decrease in BA towards the end of the experiment, which is due to the accumulation of VFA. In fact, VFA are almost completely in dissociated form (pK_a 4.76–4.88) and therefore the increased amount of H^+ ions drives the transformation of part of the BA into CO_2. In the case of GW, there is a less defined increasing trend which can be related to the lower TAN content in this system. Similarly to FW, higher loading rates corresponded to a decrease, or at least stabilization, in the BA content. BA simulations capture in both cases the experimental trends, with acceptable rAE of 10% and 5% for FW and GW, respectively. In the case of FW the simulation predicts the initial increase and the final decrease. There is a noticeable underestimation of the final experimental values, of which is difficult to identify a single cause. One possible explanation could be the inaccuracy in the experimental determination of BA. This was in fact approximated by titration to pH 5.75 and using an empirical factor to convert the measurement (partial alkalinity) to bicarbonate alkalinity (Jenkins et al., 1983). However, in systems with high concentration of TAN and VFA, the empirical factor is less accurate and BA could be overestimated: the titration in fact also converts the free ammonia to ammonium and part of the available VFA into the undissociated form. A different empirical factor could be used depending on the state of the system, but this goes beyond the scope of the research.

VFA are the main products of the fermentative and acetogenic steps; in general accumulation of VFA in the liquid phase indicates that the reaction rates of consumption of VFA (namely methanogenic reaction for acetic acid, and acetogenic reaction for propionate, butyrate and valerate) are slower than the production rates. If this imbalance is protracted in time, it can eventually lead to a failure of the whole anaerobic process, due to eventual pH drop caused by excessive concentrations of VFA. In fact, VFA have been since long accepted, alongside alkalinity, as the main

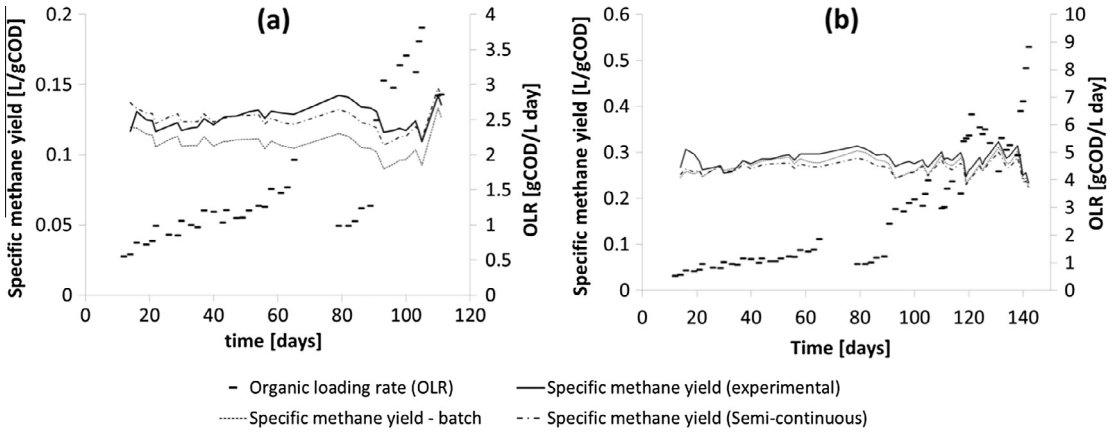

Fig. 5. Prediction of time averaged specific methane yield by (a) XS model with batch calibrated parameters and XX model with semi-continuous parameters for GW experimental data, and (b) by XX model with batch calibrated parameters and XXS model with semi-continuous parameters for FW experimental data.

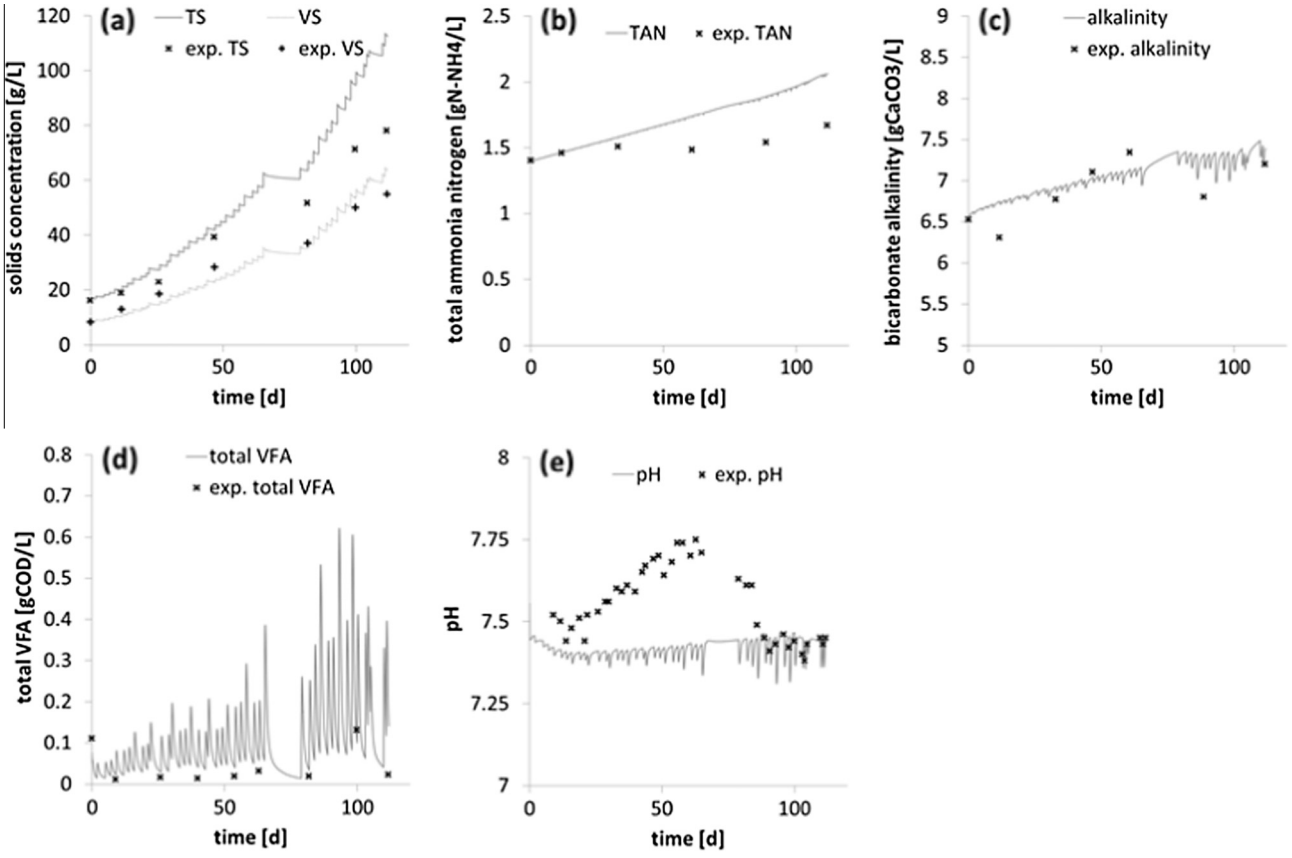

Fig. 6. Simulated (calibrated XS model) and experimental measured outputs in GW semi-continuous experiment: (a) total and volatile solids, (b) total ammonia nitrogen, (c) bicarbonate alkalinity, (d) total VFA (sum of all species), (e) pH.

indicators of process stability (Ahring et al., 1995; Boe et al., 2010). Single VFA species were measured and simulated, however the sum of all single species is here reported in Figs. 6d and 7d for GW and FW, respectively, as the focus is more on the process imbalance between acid production and consumption rates. Excluding the end period of FW test, the VFA content in the effluents remained at very low levels, with an average concentration of 0.05 gCOD L^{-1} in GW test and 0.1 gCOD L^{-1} in FW test, indicating that the applied loading rates did not cause process instability. The highest peak in GW test was 0.13 gCOD L^{-1} at 100 days, while in the case of FW a peak of 3 gCOD L^{-1} was registered. Simulations show how the spikes in VFA concentration, after each feeding, are reduced to low levels before the following feeding. Also the final accumulation of VFA in FW test is well predicted. However, the error is very high at 159% and 173% for FW and GW respectively as the simulations tend to overestimate the residual VFA. Most of the error is caused by an overestimation of the very low levels of VFA, which from an engineering and control point of view are less

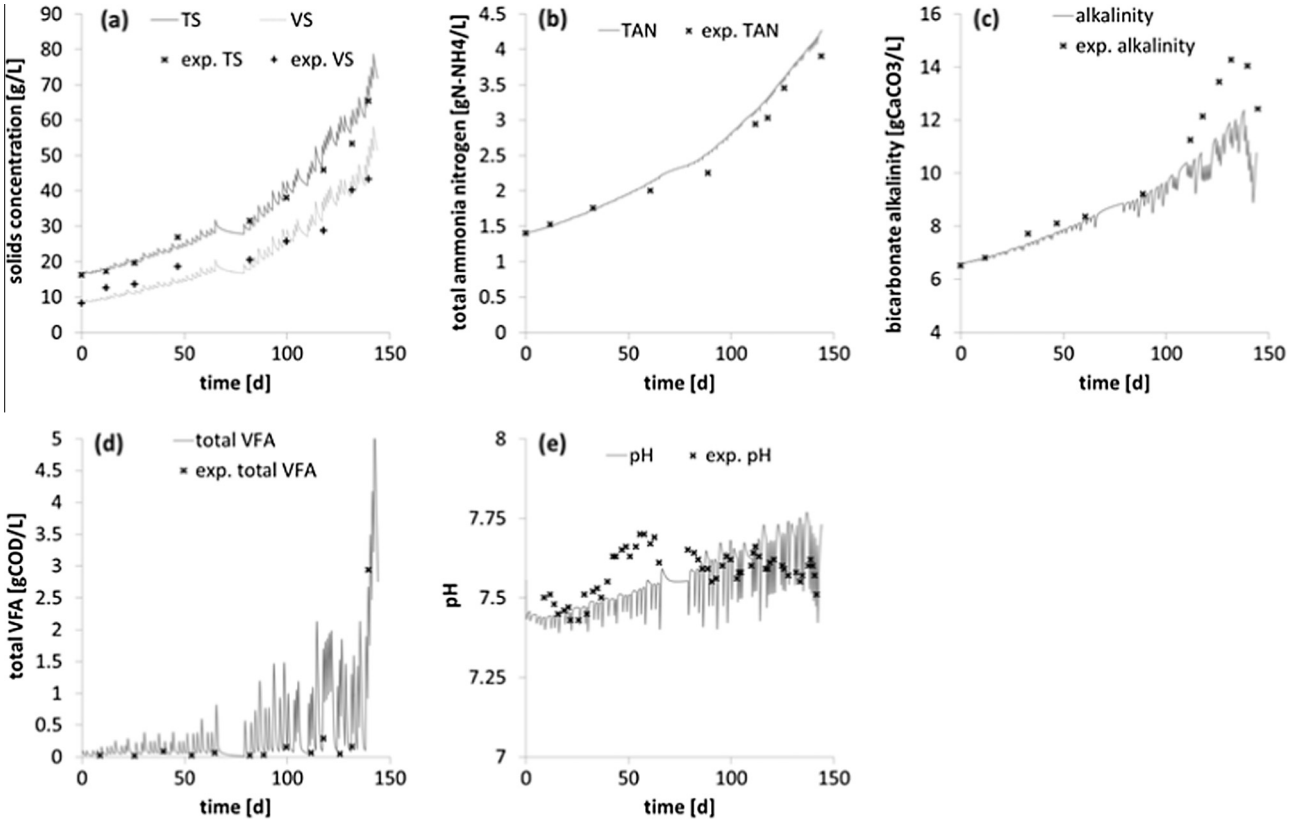

Fig. 7. Simulated (calibrated XX model) and experimental for measured outputs in FW semi-continuous experiment: (a) total and volatile solids, (b) total ammonia nitrogen, (c) bicarbonate alkalinity, (d) total VFA (sum of all species), (e) pH.

important to predict. This poor prediction can be attributed to the fact that the inhibition components of ADM1 were not modified from the default values as proposed by Rosen and Jeppsson (2006), and default inhibition mechanisms rely completely on pH, rather than the VFA themselves, as the driver of inhibition of methanogenic microorganisms.

The pH is the result of the interaction of all charge bearing species in the system. In both FW and GW semi-continuous experiments, the pH is quite stable between 7.5 and 7.75, with increasing values during the first 50 days of the experiment and then a decline and stabilization. Initial increase can be related with the observed increase in TAN concentration in the systems, with higher VFA concentrations reducing the pH in the second part of the experiment. The simulations of the pH variable, shown in Figs. 6e and 7e, tend to underestimate the pH during the initial period of the experiment, while the fit improves after 70 days in both experiments. It is difficult to identify a reason for the initial lack of fit, although it can be noticed how the implemented ADM1 cannot take into account some important influencing pH phenomena, including: phosphate buffer, sulphate-sulphide system, precipitation of carbonates (e.g. calcite $CaCO_3$), formation and precipitation of struvite. Simulations also show how the pH drops after each feeding, with the drops being proportional to the size of the feeding and related to VFA and CO_2 production which in turn increase the amount of H^+ ions in the liquid.

Methane content in the produced gas was only measured in the FW experiment, and for a limited period of time. Methane content is directly related to the biochemical composition of the substrate and in particular with the oxidation state of carbon, e.g. lipids degradation will produce a methane-richer gas than carbohydrates. At the same time, in highly dynamic systems, the gas composition also depends on the relative rates of the various biochemical reaction processes. The experimental methane content (Fig. 8a) follows remarkably well the experimental values (rAE 5%). Simulated CH_4 and CO_2 flows and their ratio are shown in Fig. 8b and it is evident how the ratio decreases abruptly after each

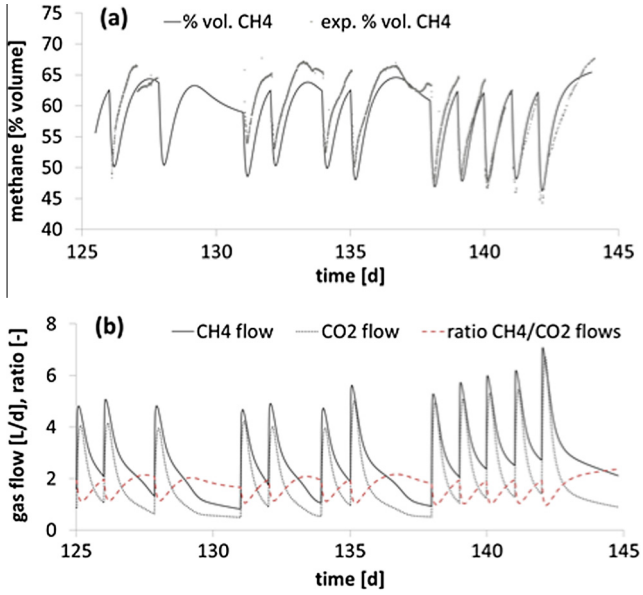

Fig. 8. (a) Simulated and experimental CH_4 content in the produced gas in FW test; (b) simulated CH_4 and CO_2 gas flow rate in FW semi-continuous test.

feeding, as the degradation of the fresh substrate initially produces a relatively high amount of CO_2 through fermentation and fatty acids oxidation. The ratio then increases again and peak, through the reduction of CO_2 to methane in hydrogenotrophic methanogenesis and the gradual conversion of the accumulated acetate to methane.

4. Conclusion

In this paper we have proposed and assessed a rigorous substrate characterisation methodology to be used with ADM1 based on a combined biochemical and kinetic fractionation approach. We have demonstrated that the prediction of methane production from complex substrates such as GW and FW by ADM1 can be improved by its modification to incorporate different particulate fractions with different degradation kinetics. Further it was shown that the quality of fit between experimental and simulated outputs increases with the number of fractions that are used represent the particulate and soluble organic matter. However, depending on the data set used to estimate the fractionation and kinetic parameters the associated parameter uncertainty may be too great to justify the more complex substrate description. It is hoped that this approach can remove some subjectivity compared with other substrate characterisation methods.

Four substrate fractionation models containing from 1 particulate (X) to 2 particulate and 1 soluble (XXS) degradable fractions were assessed and experimental methane production rate from both batch and semi-continuous experiments was used to calibrate the kinetic and fractionation parameters in each case. Using batch data the recommended fractionation models for GW and FW were XS and XX respectively, however with semi-continuous data the increased richness of the data set allowed a more complex description of the substrate, while maintaining low parameter uncertainty.

The methodology based on batch test has the advantage of being simpler and less time-consuming compared to longer semi-continuous tests. Therefore the substrate description obtained through batch tests was used to simulate the experimental data from semi-continuous test, in order to validate the methodology. The batch test methodology allowed good predictions for the methane specific yield, total and volatile solids, ammonia and alkalinity; while it was less accurate for the prediction of instantaneous methane flow rate, pH and VFA.

Acknowledgment

The authors gratefully acknowledge the support of the RCUK through the BioCPV project (EP/J000345/2).

Appendix A. Estimation of initial conditions

Microbial biomass initial conditions are difficult to determine experimentally (Jabłoński and Łukaszewicz, 2014). Usually for ADM1 implementations, a model based characterisation of the inoculum is obtained through a steady state simulation of the digester from which the inoculum is taken (Batstone et al., 2004; Girault et al., 2011). In this study, however, the description of the inoculum source digester was not sufficiently accurate to allow a useful simulation of its operation, and a combination of literature data and experimental calibration was used. Therefore the initial conditions in the batch tests were determined assuming that the measured initial theoretical COD (COD_{th}) consisted only of microorganisms, composite particulate (i.e. decayed biomass, X_c), residual degradable particulates (X_{ch}, X_{li}, X_{pr}) and inert (X_I) concentrations. It was assumed that the initial incubation period of 4 days resulted in the degradation of all of the residual soluble organic matter (S fractions) present in the fresh inoculum. The total biomass and particulate concentrations, and the hydrolysis constant of the particulate fractions were then calibrated against the measured methane production in the blank batch test; this calibration is conditional on the value of the biomass decay rate and disintegration rate of composite particulate matter, which were left at the default values. The inert fraction was found by difference from the total initial COD_{th} of the inoculum. The proportion between the trophic groups in the microbial biomass was maintained as in Rosen and Jeppsson (2006), considering that their simulation of a sludge digester was sufficiently similar to the inoculum source digester.

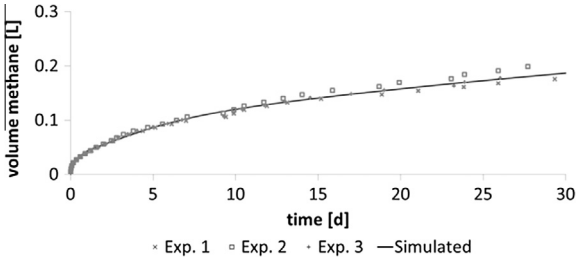

Fig. A.1. Experimental and simulated methane production for inoculum.

Table A.1
Estimated inoculum parameters for batch test.

	Estimated parameters	Units	Value	Standard error (%)
Inoculum	Initial total biomass	gCOD L^{-1}	3.12	4
	Initial decayed biomass (X_c)	gCOD L^{-1}	0.89	57
	Initial total degradable particulate	gCOD L^{-1}	0.42	26
	Hydrolysis rate of initial particulate	d^{-1}	0.39	15

Table A.1 shows the estimated parameters for the description of the inoculum, and Fig. A.1 the experimental and calibrated methane volume production curves from the control reactors in batch test. Estimated parameters have very high standard errors, especially in the case of total particulate and decayed biomass X_c (>50% for X_c), due to their almost complete correlation (>0.99, results not shown), while errors in biomass concentrations are lower (<5% in both cases). In both cases the goodness of fit was very high (R^2 = 99%). Alternative tests were performed by calibrating less parameters (e.g. with X_c at a fixed value), but achieving lower goodness of fit. In the simulation of substrate batch tests, the methane production is the result of the degradation of the substrate together with the inoculum: therefore an accurate kinetic characterisation of the substrate is dependent on an accurate description of the degradation of the inoculum. For this reason, although poorly identifiable, the estimated parameters were accepted as the initial conditions of the tests.

References

Abbassi-Guendouz, A., Brockmann, D., Trably, E., Dumas, C., Delgenès, J.-P., Steyer, J.-P., Escudié, R., 2012. Total solids content drives high solid anaerobic digestion via mass transfer limitation. Bioresour. Technol. 111, 55–61.

Ahring, B.K., Sandberg, M., Angelidaki, I., 1995. Volatile fatty acids as indicators of process imbalance in anaerobic digestors. Appl. Microbiol. Biotechnol. 43 (3), 559–565.

APHA, 2005. Standard Methods for the Examination of Water and Wastewater. American Public Health Association (APHA), Washington, DC, USA.

Astals, S., Esteban-Gutiérrez, M., Fernández-Arévalo, T., Aymerich, E., García-Heras, J.L., Mata-Alvarez, J., 2013. Anaerobic digestion of seven different sewage sludges: a biodegradability and modelling study. Water Res. 47 (16), 6033–6043.

Baker, J.R., Milke, M.W., Mihelcic, J.R., 1999. Relationship between chemical and theoretical oxygen demand for specific classes of organic chemicals. Water Res. 33 (2), 327–334.
Batstone, D., Puyol, D., Flores-Alsina, X., Rodríguez, J., 2015. Mathematical modelling of anaerobic digestion processes: applications and future needs. Rev. Environ. Sci. Biotechnol., 1–19
Batstone, D., Torrijos, M., Ruiz, C., Schmidt, J., 2004. Use of an anaerobic sequencing batch reactor for parameter estimation in modelling of anaerobic digestion. Water Sci. Technol. 50 (10), 295–303.
Batstone, D.J., 2013. Modelling and control in anaerobic digestion: achievements and challenges. In: 13th World Congress on Anaerobic Digestion. International Water Association (IWA).
Batstone, D.J., Keller, J., Angelidaki, I., Kalyuzhnyi, S.V., Pavlostathis, S.G., Rozzi, A., Sanders, W.T.M., Siegrist, H., Vavilin, V.A., 2002. The IWA Anaerobic Digestion Model No 1 (ADM1). Water Sci. Technol. 45 (10), 65–73.
Batstone, D.J., Tait, S., Starrenburg, D., 2009. Estimation of hydrolysis parameters in full-scale anerobic digesters. Biotechnol. Bioeng. 102 (5), 1513–1520.
Boe, K., Batstone, D.J., Steyer, J.-P., Angelidaki, I., 2010. State indicators for monitoring the anaerobic digestion process. Water Res. 44 (20), 5973–5980.
Dochain, D., Vanrolleghem, P., 2001. Dynamical Modelling and Estimation in Wastewater Treatment Processes. IWA Publishing.
ECN/Phyllis. Phyllis – Database for Biomass and Waste, Energy Research Centre of the Netherlands.
García-Gen, S., Sousbie, P., Rangaraj, G., Lema, J.M., Rodríguez, J., Steyer, J.-P., Torrijos, M., 2015. Kinetic modelling of anaerobic hydrolysis of solid wastes, including disintegration processes. Waste Manage. 35, 96–104.
Gerloff, E.D., Lima, I.H., Stahmann, M.A., 1965. Leaf proteins as foodstuffs, amino acid composition of leaf protein concentrates. J. Agric. Food Chem. 13 (2), 139–143.
Girault, R., Bridoux, G., Nauleau, F., Poullain, C., Buffet, J., Steyer, J.P., Sadowski, A.G., Béline, F., 2012. A waste characterisation procedure for ADM1 implementation based on degradation kinetics. Water Res. 46 (13), 4099–4110.
Girault, R., Rousseau, P., Steyer, J., Bernet, N., Beline, F., 2011. Combination of batch experiments with continuous reactor data for ADM1 calibration: application to anaerobic digestion of pig slurry. Water Sci. Technol. 63 (11), 2575–2582.
Gujer, W., 2008. Systems Analysis for Water Technology. Springer Science & Business Media.
Jabłoński, S.J., Łukaszewicz, M., 2014. Mathematical modelling of methanogenic reactor start-up: importance of volatile fatty acids degrading population. Bioresour. Technol. 174, 74–80.
Jenkins, S.R., Morgan, J.M., Sawyer, C.L., 1983. Measuring anaerobic sludge digestion and growth by a simple alkalimetric titration. Journal (Water Pollut. Control Fed.) 55 (5), 448–453.
Jensen, P.D., Hardin, M.T., Clarke, W.P., 2009. Effect of biomass concentration and inoculum source on the rate of anaerobic cellulose solubilization. Bioresour. Technol. 100 (21), 5219–5225.
Kleerebezem, R., Van Loosdrecht, M.C.M., 2006. Waste characterization for implementation in ADM1. Water Sci. Technol. 54 (4), 167–174.
Koch, K., Lubken, M., Gehring, T., Wichern, M., Horn, H., 2010. Biogas from grass silage – measurements and modeling with ADM1. Bioresour. Technol. 101 (21), 8158–8165.
Lübken, M., Wichern, M., Schlattmann, M., Gronauer, A., Horn, H., 2007. Modelling the energy balance of an anaerobic digester fed with cattle manure and renewable energy crops. Water Res. 41 (18), 4085–4096.
Mottet, A., Ramirez, I., Carrère, H., Déléris, S., Vedrenne, F., Jimenez, J., Steyer, J.P., 2013. New fractionation for a better bioaccessibility description of particulate organic matter in a modified ADM1 model. Chem. Eng. J. 228, 871–881.
Myer, R., Brendemuhl, J., Johnson, D., 2000. Dehydrated restaurant food waste as swine feed. Food Waste Anim. Feed, 113–144.
Noguerol-Arias, J., Rodríguez-Abalde, A., Romero-Merino, E., Flotats, X., 2012. Determination of chemical oxygen demand in heterogeneous solid or semisolid samples using a novel method combining solid dilutions as a preparation step followed by optimized closed reflux and colorimetric measurement. Anal. Chem. 84 (13), 5548–5555.
Nopens, I., Batstone, D.J., Copp, J.B., Jeppsson, U., Volcke, E., Alex, J., Vanrolleghem, P. A., 2009. An ASM/ADM model interface for dynamic plant-wide simulation. Water Res. 43 (7), 1913–1923.
Ralston, M.L., Jennrich, R.I., 1978. DUD, a derivative-free algorithm for nonlinear least squares. Technometrics 20 (1), 7–14.
Raposo, F., de la Rubia, M.A., Borja, R., Alaiz, M., 2008. Assessment of a modified and optimised method for determining chemical oxygen demand of solid substrates and solutions with high suspended solid content. Talanta 76 (2), 448–453.
Raposo, F., De La Rubia, M.A., Fernandez-Cegri, V., Borja, R., 2012. Anaerobic digestion of solid organic substrates in batch mode: an overview relating to methane yields and experimental procedures. Renew. Sustain. Energy Rev. 16 (1), 861–877.
Reichert, P., 1998. AQUASIM 2.0 – User Manual. Swiss Federal Institute for Environmental Science and Technology, Dubendorf, Switzerland.
Ripley, L.E., Boyle, W.C., Converse, J.C., 1986. Improved alkalimetric monitoring for anaerobic digestion of high-strength wastes. Journal (Water Pollut. Control Fed.) 58 (5), 406–411.
Rittmann, B.E., McCarty, P.L., 2001. Environmental Biotechnology. McGraw-Hill, Boston.
Rodríguez-Abalde, Á., Juznic, Z., Fernández, B., Flotats, X., 2013. Anaerobic disintegration of agro-industrial organic waste. Reliability of Parameters Identification. In: World Congress on Anaerobic Digestion, p. IWA-10856.
Rosen, C., Jeppsson, U., 2006. Aspects on ADM1 Implementation within the BSM2 Framework. Department of Industrial Electrical Engineering and Automation, Lund University, Lund, Sweden.
Solon, K., Flores-Alsina, X., Gernaey, K.V., Jeppsson, U., 2015. Effects of influent fractionation, kinetics, stoichiometry and mass transfer on CH_4, H_2 and CO_2 production for (plant-wide) modeling of anaerobic digesters. Water Sci. Technol. 71 (6), 870–877.
Souza, T.S., Carvajal, A., Donoso-Bravo, A., Pena, M., Fdz-Polanco, F., 2013. ADM1 calibration using BMP tests for modeling the effect of autohydrolysis pretreatment on the performance of continuous sludge digesters. Water Res. 47 (9), 3244–3254.
Steyer, J., Bernard, O., Batstone, D., Angelidaki, I., 2006. Lessons learnt from 15 years of ICA in anaerobic digesters. Water Sci. Technol. 53 (4–5), 25–33.
Strömberg, S., Nistor, M., Liu, J., 2014. Towards eliminating systematic errors caused by the experimental conditions in Biochemical Methane Potential (BMP) tests. Waste Manage. 34 (11), 1939–1948.
Taylor, J.R., 1996. An Introduction to Error Analysis: The Study of Uncertainties in Physical Measurements. University Science Books, Sausalito, California.
Thamsiriroj, T., Murphy, J.D., 2011. Modelling mono-digestion of grass silage in a 2-stage CSTR anaerobic digester using ADM1. Bioresour. Technol. 102 (2), 948–959.
Vavilin, V.A., Fernandez, B., Palatsi, J., Flotats, X., 2008. Hydrolysis kinetics in anaerobic degradation of particulate organic material: an overview. Waste Manage. 28 (6), 939–951.
Wichern, M., Gehring, T., Fischer, K., Andrade, D., Lübken, M., Koch, K., Gronauer, A., Horn, H., 2009. Monofermentation of grass silage under mesophilic conditions: measurements and mathematical modeling with ADM 1. Bioresour. Technol. 100 (4), 1675–1681.
Yasui, H., Goel, R., Li, Y.Y., Noike, T., 2008. Modified ADM1 structure for modelling municipal primary sludge hydrolysis. Water Res. 42 (1–2), 249–259.
Zaher, U., Buffiere, P., Steyer, J.P., Chen, S., 2009. A procedure to estimate proximate analysis of mixed organic wastes. Water Environ. Res. 81 (4), 407–415.